

Characterization of a Viking Blade Fabricated by Traditional Forging Techniques

H. VO,^{1,5,7} D. FRAZER,¹ N. BAILEY,¹ R. TRAYLOR,² J. AUSTIN,⁴
J. PRINGLE,⁴ J. BICKEL,¹ R. CONNICK,¹ W. CONNICK,³
and P. HOSEMANN^{1,6,8}

1.—Department of Nuclear Engineering, University of California Berkeley, Etcheverry Hall, Berkeley, CA 94720, USA. 2.—Department of Materials Science and Engineering, University of California Berkeley, Hearst Mining Hall, Berkeley, CA 94720, USA. 3.—Department of Mechanical Engineering, University of California Berkeley, Etcheverry Hall, Berkeley, CA 94720, USA. 4.—Alchemy Metalworks, 2440 Adeline, Oakland, CA, USA. 5.—2111A Etcheverry Hall, Berkeley, CA 94720, USA. 6.—4169 Etcheverry Hall, Berkeley, CA 94720, USA. 7.—e-mail: sfhivo@berkeley.edu. 8.—e-mail: peterh@berkeley.edu

A team of students from the University of California, Berkeley, participated in a blade-smithing competition hosted by the Minerals, Metals, and Materials Society at the TMS 2015 144th annual meeting and exhibition. Motivated by ancient forging methods, the UC Berkeley team chose to fabricate our blade from historical smithing techniques utilizing naturally-occurring deposits of iron ore. This approach resulted in receiving the “Best Example of a Traditional Blade Process/Ore Smelting Technique” award for our blade named “Berkelium.” First, iron-enriched sand was collected from local beaches. Magnetite (Fe_3O_4) was then extracted from the sand and smelted into individual high- and low-carbon steel ingots. Layers of high- and low-carbon steels were forge-welded together, predominantly by hand, to form a composite material. Optical microscopy, energy dispersive spectroscopy, and Vickers hardness mechanical testing were conducted at different stages throughout the blade-making process to evaluate the microstructure and hardness evolution during formation. It was found that the pre-heat-treated blade microstructure was composed of ferrite and pearlite, and contained many nonmetallic inclusions. A final heat treatment was performed, which caused the average hardness of the blade edge to increase by more than a factor of two, indicating a martensitic transformation.

BACKGROUND

The Iron Age is generally thought to have initiated sometime between 1200 BC and 1000 BC.¹ However, Sherby et al. Ref. 2 proposed that the use of iron tools and weaponry may date as far back as 7000 BC, which precedes the Bronze Age. An evaluation of the history of iron-based blacksmithing provides an appreciation of the significant progress that has been made in metallurgy. As such, the UC Berkeley blade-smithing team decided to incorporate some of this history into our blade by mimicking ancient blade-forging techniques and methodology when feasible. Overall, Berkelium was modeled after a single-edge Viking style blade

from about 800 AD and utilized various traditional forging and iron-making techniques common to that time.

In order to produce a truly Californian blade, a locally-sourced iron ore source was used. The northern Californian beaches around San Francisco often contain large amounts of magnetite,³ which originates in the Sierra Nevada Mountains and is transported to the coast via the Sacramento and San Joaquin rivers.^{3–5} Iron-enriched sand has been used as an iron source throughout ancient history. For example, Japanese traditional blade steel, or *tamahagane*, was produced by refining the so-called “black sands,” also known as *satetsu*.^{6,7} Similar to traditional techniques, the magnetite in our sand

was separated from the other constituents. We, however, had the luxury of using neodymium magnets for this separation; former blacksmiths did not. The magnetite was then added into a crucible with a dry mixture of crushed charcoal, CaCO_3 , and glass. It was then reduced in a furnace into a carbon-enriched iron ingot and slag. This process was similar in manner to the traditional Japanese process called *tatara*. However, in our work, we utilized a natural gas-fired home-built blast furnace instead of the traditional furnaces used in 800 AD.

The texture of our blade was inspired by the laminated composite and pattern-welded techniques that have been universally used by blacksmiths throughout history.⁷ The history of laminated composite metals dates back to antiquity and the first historical account of its usage is seen in Homer's *The Iliad*.⁸ This account describes Achilles' shield as consisting of two external bronze layers, two internal tin layers, and one gold layer. Another example of laminated metallic composites was demonstrated by adze blades, produced by Greek blacksmiths circa 400 BC.⁷ The adzes contained both high and low carbon steels in order to improve mechanical performance of the blades.

There are several factors that contribute to the attractiveness of laminated composite structures (LCS). Since carburization of large work pieces can be difficult, high-carbon steel could only be produced in small quantities. Using LCS, small pieces of high-carbon steel can be folded into layers of low-carbon steel. This allows a blade to achieve the beneficial properties of both constituent materials. For example, in a traditional Japanese *katana* sword, the lamination of steel pieces of varying carbon contents produced better toughness, hardness, and strength in the sword as a whole.⁷ Lastly, laminating forged-welded pieces of steel yields visibly entrancing patterns on the blade's surface.

SWORD MAKING PROCESS

Proper personal protective equipment included safety goggles, closed steel-toed shoes, long pants, and heat-resistant gloves were worn at all times during the smelting/forging process. When handling and working on the work pieces, leather clothing and a face shield were also required, as ejection and splashing of hot particulates can occur. Furthermore, at all times, the two-man rule applied so that no single person was working on the blade alone.

Starting Material

As previously discussed, the steel used for the blade was fabricated from naturally-occurring iron ores. Due to the strong affinity between Fe and O, iron ore is generally found in the form of iron oxide, such as hematite (Fe_2O_3) or magnetite (Fe_3O_4). These ores are also known to contain

varying quantities of other impurity elements such as Si, S, Mn, and P. Since magnetite has a higher iron-to-oxygen ratio than hematite, it is more magnetic than hematite. This allowed for easy segregation of magnetite from the other elements and compounds in the sand via neodymium magnets. The concentration of magnetite varies between beaches but is especially abundant along strongly eroded areas along the northern California Pacific coast.³ Sieving of the sand prior to magnetite separation was performed with a metal strainer to separate out large particles, plant matter rocks, and trash in an effort to reduce the overall impurity content in the smelted steel ingot. Impurities and inclusions can have deleterious effects on the mechanical performance of the steel as they act as stress concentrators and crack-nucleation sites.

Smelting to Produce Steel

Smelting is the process by which a metal ore is reduced to a metal, via chemical reaction(s) at high temperature. The smelting process was implemented by the UC Berkeley blade-smithing team for the production of two high-carbon ingots and three low-carbon ingots. It began with a homogeneous dry mixture of 1200 g (75 wt.%) magnetite, 200 g (12.5 wt.%) crushed charcoal, and 200 g (12.5 wt.%) calcium carbonate (CaCO_3), contained within a graphite/clay crucible and topped with a broken-glass (SiO_2). Since silica is a natural impurity in the sand ore, no exact weight of the silica charged to the furnace was recorded. However, ~90 g of broken glass was added to the smelt. A home-made natural gas-fired rudimentary blast furnace was formed by refractory wrapping ceramic wool around a 12-in (~305-mm) pipe set atop clay firebricks, and then removing the pipe. The smelter is 12 in (~305 mm) in diameter, and 24 in (~610 mm) in height. A schematic of the furnace is shown in Fig. 1a.

The graphite/clay crucible was selected since it could withstand the intense temperatures necessary for smelting. It should also be noted that the crucible itself likely acted as a secondary carbon source, in addition to the added charcoal, during the reduction process. The consistency (when melting occurred) of the smelt was checked periodically during the smelting process with an iron rod. It was found that the minimum required time for melting to commence was approximately 45 min to 1 h. The peak temperature in the furnace was approximately 1600°C. The flux agents, CaCO_3 and glass, were added to the initial dry mixture to help further reduce the amount of impurities accompanying the iron ore by reacting with the rock gangue to produce slag. Slag is mixture of oxides that float on top of the molten iron and serve to protect the melt from the environment (i.e. oxidation of the metallic iron) during the smelting and cooling processes.

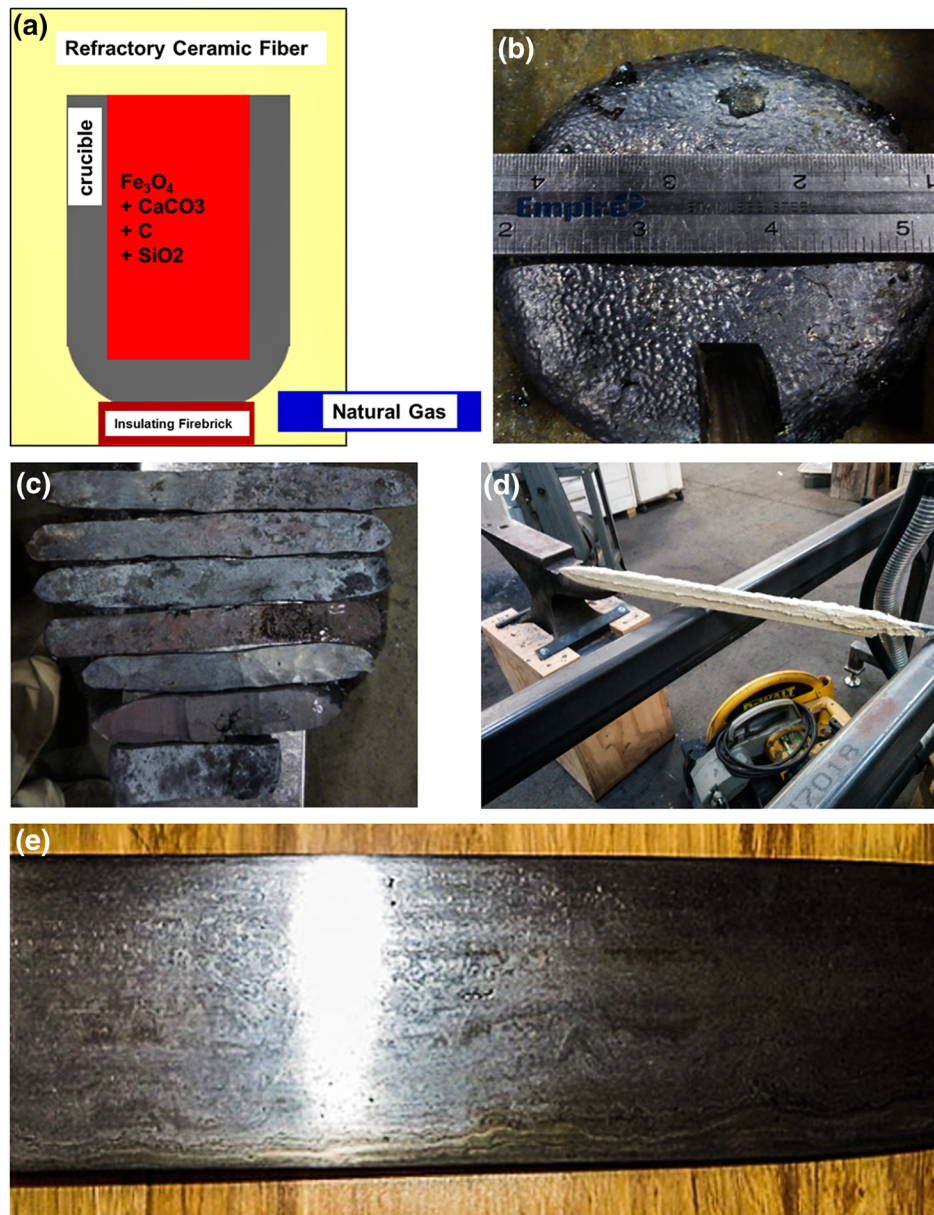


Fig. 1. (a) Furnace schematic. (b) An ingot from one of the smelt. (c) Hand-forged strips for the forge -welding. (d) Plaster coating prior to quenching. (e) Final blade surface showing forge welding pattern.

After the smelting, the result was a porous mass of a ~ 3.3 -in (~ 84 -mm)-diameter iron-carbon alloy ingot (Fig. 1b) and slag. It was observed that 1200 g of magnetite formed approximately 800 g solid metal by this smelting process, which was repeated five times to create approximately 4 kg of steel. A rough estimate of the relative carbon contents for each ingot was quantified via spark testing.⁹ Spark testing estimates the carbon content in steel according to the shape and size of the sparks generated during abrasive grinding. It was found that the different ingots did indeed show different carbon contents according to this testing method. At this

stage in the blade manufacturing process, the ingots were classified qualitatively as either high and low carbon until more analyses could be performed.

Forging

The as-smelted ingots were then separated into groups based on carbon content: two high-carbon ingots and three low-carbon ingots in total. Each ingot was cut into three equal segments using a high-speed saw. All 15 segments were then hand-forged into long, thin strips by students in alternating teams of three, as shown in Fig. 1c. Repetitive

heating, hammering, and sprinkling of additional flux powder (borax) onto the work piece were performed. These steps helped to drive out large slag inclusions, prevent excess oxidation during forging, homogenize the microstructure, and reduce overall porosity. Once formed, the hand-forged pieces were then shaped into equal rectangular billets with a power hammer. The four billets were then forge welded into a larger faggot, which was drawn out lengthwise and cut into three pieces. The faggoting process was repeated three times for the low carbon pieces resulting in a total of 36 folds. However, the high carbon billets, which were limited by the amount of smelted material, were faggoted only twice, yielding 12 folds. One high-carbon piece was sandwiched between two low-carbon pieces and then forge-welded together using a power hammer. The resulting unified metallic laminate of 84 folds was then ready to be shaped into a blade. The laminate was drawn out into a rough blade shape with a width of ~ 1.2 in (~ 31.8 mm) and a length ~ 2 feet (~ 610 mm). The tip of the blade was formed by hand by carefully striking the heated tip at an angle on both sides, and blacksmithing leveler and striker tools were used to form the sharp cutting edge of the blade. The handle end of the blade, also known as the tang, was also formed by hand. The as-forged blade was cleaned of surface oxides and ground into its final shape using a sand blaster and belt sander, respectively.

Heat-Treating and Hardening the Sword

Once the final shape was obtained, the blade was coated in a plaster mix composed of fire clay, grog (crushed pottery and firebricks), and cellulose fiber (Fig. 1d). The source of cellulose fiber is from paper-making pulp, called linter. A thinner coating was applied to the cutting edge to control cooling rates and allow for a locally more rapid quench, which was predicted to create a hard martensite cutting edge. Conversely, the thicker coating along the rest of the blade was intended to prevent the martensitic transformation from occurring elsewhere during the quench, leaving the body of the blade with higher ductility and toughness. Once coated with this plaster mixture, the blade was then heated to 800°C (above the austenization temperature), held for 15 min, and quenched in oil to room temperature. Following the oil quench, the blade was tempered in a conventional oven at 200°C for 1 h to relieve residual internal stresses, and improve elasticity of the blade in general. Finally, after hardening and tempering, the blade was polished and lightly etched with Nital (3% nitric acid) etching solution to illuminate the laminating pattern produced by the forge welding. The final blade with the forge welding pattern is shown in Fig. 1e.

MATERIALS CHARACTERIZATION

During the processing described above, several samples were collected from the material. The smaller pieces of steel were mounted in cold-mount epoxy, ground with silicon carbide paper, and polished with a $1\text{-}\mu\text{m}$ diamond suspension. Subsequent microscopy analysis was performed using a Zeiss optical microscope as well as scanning electron microscopy (SEM) using a Quanta 3D FEG. The Quanta is also equipped with an Oxford Energy Dispersive Spectroscopy (EDS) detector to identify the elements present in the material.

The as-smelted sample showed that the material was indeed iron and carbon but also contained numerous inclusions. EDS analysis provided details on the inclusion composition, summarized in Fig. 2a. It was concluded that the inclusions were non-metallic due to their high phosphorous and sulfur contents. This is supported by the fact that phosphates and sulfides are common impurities found in iron ores and surely would have been included in the collected beach sand. Chromium, sulfur and vanadium appear to be confined within the inclusion whereas phosphorous and carbon are more diffuse. The detection of silicon could be from the sand itself. Optical microscopy revealed that perlite and ferrite are present in the material, indicated in Fig. 2b.

A similar analysis was also performed on a sample acquired after the low- and high-carbon pieces were laminated together but prior to forge welding into a single billet. Large inclusions for both high- and low-carbon pieces were observed. However, the lower-carbon side contained more inclusions than the higher-carbon side, which may be a consequence of the shorter smelting time. A ferrite + pearlite microstructure was observed for the high-carbon piece whereas the low-carbon region was shown to be predominately ferrite. Figure 2c shows an optical micrograph of the low-carbon (left) and high-carbon (right) interface after etching. An SEM image of the high-carbon region confirms the presence of pearlite + ferrite, as shown in Fig. 2d.

Ten Vickers hardness indents were made in each of the low- and high-carbon region. It was found that the low-carbon region and high-carbon region had a Vickers hardness of 138 ± 16 HV and 210 ± 31 HV, respectively. We attribute the higher hardness of the high-carbon region to the presence of ferrite plus a larger amount of pearlite, which is promoted by the higher carbon content. It is important to note that the hardness measurements of the high-carbon region had a higher standard deviation than the low-carbon region. This could be due to several reasons including uneven distribution of carbon throughout the piece, the size and distribution of the pearlitic microstructure, and the reduced number of overall inclusions as compared to the low-carbon region.

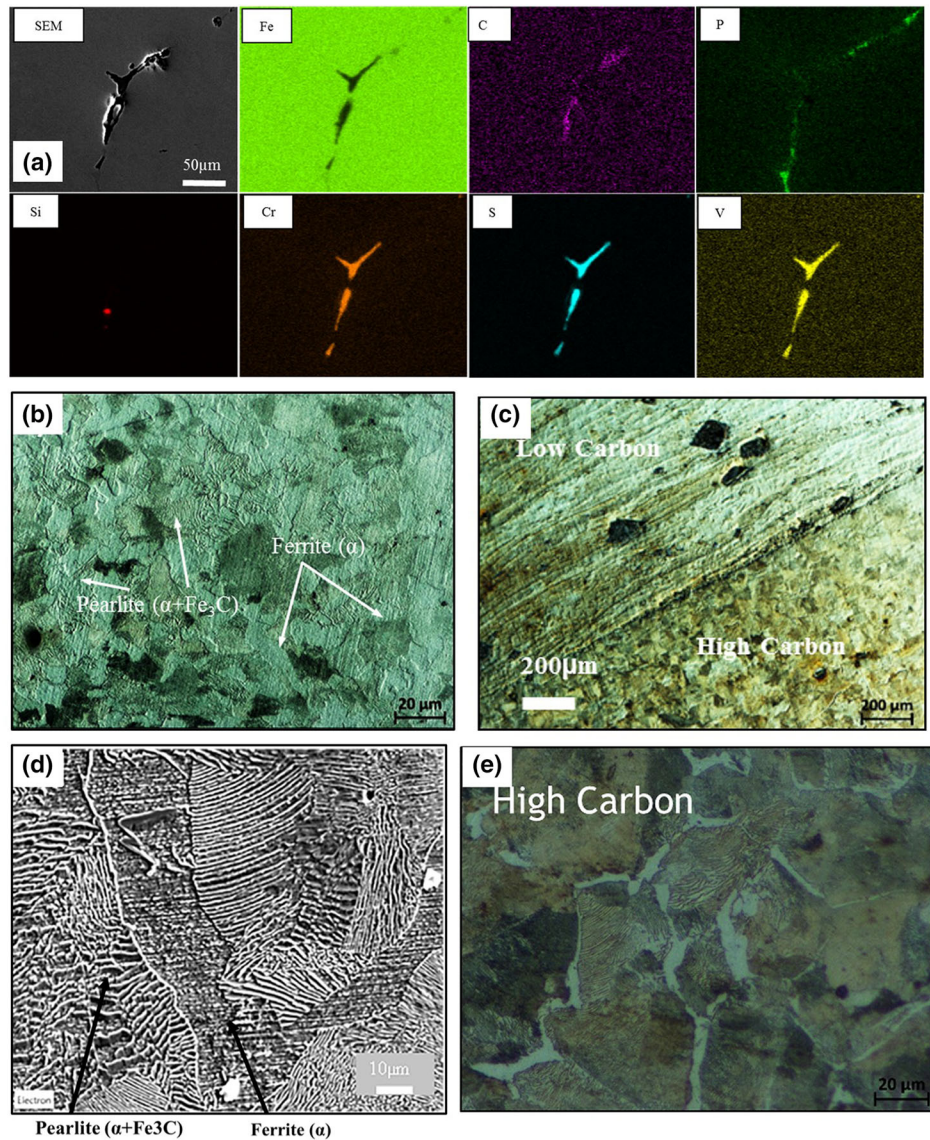


Fig. 2. (a) EDS analysis of an inclusion of the as-smelted ingot. (b) OM image of a low-carbon ingot. (c) OM image of the laminated composite after etching. (d) SEM image of the high-carbon region of the laminate composite. (e) OM image of high-carbon region used for carbon content determination.

The last round of analysis was conducted on the blade after it was forged into its final shape. The surfaces of these samples were shown to have finer inclusions, but similar chemical compositions as the laminated composite. Also, the inclusions were aligned parallel to the long axis of the blade. Digital image analysis was performed on optical micrographs after etching in order to determine the carbon content of each region (Fig. 2e). By applying a grayscale filter to the images, the pearlite can be separated from the ferrite and therefore the amount of pearlite versus ferrite can be estimated. The carbon content of the high-carbon and low-carbon pieces were calculated to be roughly 0.7% and 0.26%, respectively. Vickers hardness testing was performed on these samples, where it was found

that lower-carbon and higher-carbon regions had an average hardness of 140 ± 9 HV and 288 ± 24 HV, respectively.

High-magnification optical and electron micrographs and chemical analysis of the final blade itself were not possible as it was too large to fit into an SEM and optical microscopes without cutting. Therefore, the presence of martensite by the sharp edge of the blade could not be confirmed by microscopy. However, the hardness measurements showed that the heat treatment significantly increased hardness from 140 ± 9 HV to 467 ± 130 HV in the low-carbon region and from 288 ± 24 HV to 699 ± 185 HV in the high-carbon region, suggesting that a martensitic transformation had occurred.

DISCUSSION

The final blade consists of a high-carbon core sandwiched between two layers of low-carbon steels. The reasoning behind integrating two different carbon-content steels was to combine the high strength and hardness from the high-carbon steel with the high toughness and ductility from the low-carbon steel. However, the higher density of inclusions in the low-carbon steel likely reduced its overall toughness and mechanical performance since they serve as stress-concentration sites for crack initiation and propagation. Large inclusion particles consisting of silicon, manganese, calcium, and other oxides were found in both the high-carbon and low-carbon materials and it is believed their presence is due to contamination from the ore. Since it was found that the higher-carbon steel contained fewer inclusions, we conclude that a combination of increasing smelt time (to produce higher-carbon steel) and decarburizing during the forging process will produce higher-quality steel for the sword fabrication.

Before heat treatment, a ferrite + pearlite structure was found in both the low-carbon and high-carbon steels after quenching, though the low-carbon steel was predominantly composed of ferrite with very little pearlite. Additionally, the formation of martensite was inferred on the blade edge due to the significant increase in hardness. It is believed that the grain size, carbon content, and microstructure contributed to the difference in hardness values of the samples. The blade's microhardness was 140 ± 9 HV in the low-carbon region and 288 ± 24 HV in the high-carbon region prior to the hardening heat treatment. After hardening, the average hardness of the blade edge increased to 699 ± 185 HV in the high-carbon region and 467 ± 130 HV in the low-carbon region. However, due to inhomogeneities in chemical composition, microstructural texture, and potentially uneven heating during the heat treatment throughout the blade edge, the microhardness value varies significantly between different regions. It was found that our measured hardness values do fall within the expected range upon heat treatment. According to Grange et al. Ref. ¹⁰, it was found that after quenching and annealing, a hardness of ~ 700 HV was reported on a 0.7 wt.% C piece of steel, while a hardness of ~ 450 HV was reported after the same treatment on a 0.27 wt.% C piece of steel.

CONCLUSION

The UC Berkeley 2015 blade-smithing team designed and fabricated Berkelium, a locally produced and sourced sword, under the guidance of James Austin. The blade shape of Berkelium was modeled after a simple single-edge Viking style blade from about 800 AD. In addition, we successfully created a laminated and functional graded material that is comparable to ancient Viking blades. A number of large inclusions were found in the homemade material, but this was a common problem for European blacksmiths in 800 AD. There is potential for improving the process by producing higher-carbon material since there appears to be fewer inclusions in the higher-carbon part of the blade. Despite the quality of our homemade steel, the fact that the UC Berkeley blade-smithing team was able to manufacture a sword from iron-enriched sand, locally collected from a publically-accessible beach, was a true achievement. Though the sword-making process was extremely time- and labor-intensive, participating in this project proved to be a personally enriching experience for all participants. All of our hard work was publically recognized at the TMS 2015 blade-smithing competition when we were awarded the title "Best Example of a Traditional Blade Process/Ore Smelting Technique." As a result, we eagerly look forward to the next blade-smithing competition.

ACKNOWLEDGEMENTS

We would like to acknowledge The Minerals, Metals, and Materials Society for hosting the 2015 Bladesmithing competition.

REFERENCES

1. J. Wadsworth, *Mater. Charact.* 99, 1 (2015).
2. O.D. Sherby and J. Wadsworth, *J. Mater. Process. Technol.* 117, 347 (2001).
3. P.L. Barnard, A.C. Foxgrover, E.P.L. Elias, L.H. Erikson, J.R. Hein, M. McGann, K. Mizell, R.J. Rosenbauer, P.W. Swarzenski, R.K. Takesue, F.L. Wong, and D.L. Woodrow, *Mar. Geol.* 336, 120 (2013).
4. S.A. Wright and D.H. Schoellhamer, *San Franc. Estuary Watershed Sci.* 2, Article 2 (2004).
5. D.H. Schoellhamer, *Estuaries Coasts* 34, 885 (2011).
6. C. Matsumoto, A.K. Das, T. Ohba, S. Morito, T. Hayashi, and G. Takami, *J. Alloys Compd.* 577, S673 (2013).
7. J. Wadsworth and D.R. Lesuer, *Mater. Charact.* 45, 289 (2000).
8. S.A. Paipetis and V. Kostopoulos, in *Sci. Technol. Homeric Epics*, edited by S.A. Paipetis (Springer Netherlands, Dordrecht, 2008), pp. 181–203.
9. R.W. Buzzard, *Bur. Stand. Res. Paper No RP-605* (1933).
10. R.A. Grange, C.R. Hribal, and L.F. Porter, *Metall. Trans. A* 8, 1775 (1977).